Contribution from the Department of Chemistry,
Michigan State University, East Lansing, Michigan 48824

Intercalation of Metal Cluster Complexes in Smectite Clay

EMMANUEL P. GIANNELIS and THOMAS J. PINNAVAIA*

Received February 11, 1985

The cationic metal cluster complexes $Ru_3(CO)_9(P\text{–}P^+)_3$, $H_4Ru_4(CO)_8(P\text{–}P^+)_4$, $Ir_4(CO)_9(P\text{–}P^+)_3$, $Os_3(CO)_{11}(P\text{–}P^+)$, and $H_2Os_3(CO)_{10}(P\text{–}P^+)$, where $P\text{–}P^+$ is the phosphonium–phosphine ligand $Ph_2P(CH_2)_2P^+Ph_2(CH_2Ph)$, have been synthesized as BF_4^- salts. On the basis of similarities in IR carbonyl stretching frequencies, the cationic complexes are structurally analogous to neutral analogues containing arylphosphine ligands. The ion-exchange reaction of Na^+–hectorite, a typical smectite clay, in aqueous suspension with solutions of the cationic clusters in acetone results in the formation of cluster–clay intercalation compounds with d_{001} spacings in the range 22–27 Å and gallery heights of 12.5–17.5 Å. $H_2Os_3(CO)_9(P\text{–}P^+)$–hectorite, which is formed from $H_2Os_3(CO)_{10}(P\text{–}P^+)$–hectorite by thermal decarbonylation, is the first known example of an intercalated metal cluster catalyst. The longevity of the intercalated cluster for the isomerization of 1-hexene is similar to that of the homogeneous cluster, with approximately 3300 turnovers of the cluster being observed before cessation of activity due to the formation of a coordinatively saturated $H_2Os_3(CO)_9$(vinylidene)$(P\text{–}P^+)$ species.

Introduction

Metal cluster carbonyl complexes have been regarded as mimics of metal aggregates in chemisorption and complex catalytic processes.[1,2] Also, metal cluster complexes have been converted into catalytically useful heterogeneous analogues by immobilization to functionalized polymers and refractory metal oxides.[3-9] In addition, the immobilized clusters can be decarbonylated or oxidized to form catalysts with more or less uniformly dispersed metal[10,11] or metal oxide aggregates.[12] However, the immobilization of metal clusters on functionalized surfaces is not without disadvantages. For instances, the reaction of metal clusters with phosphine-functionalized supports can lead to a distribution of products with different degrees of phosphine substitution.[3,13]

Swelling layered silicate clays, such as hectorite or montmorillonite, offer an alternative to amorphous polymers and oxides for the immobilization of metal complexes.[14] Cationic complexes often can be intercalated between the silicate layers without loss of structural integrity, and the interlayers can be swelled to allow ready access of substrate molecules to the solution-like intracrystalline environment. In addition, the effect of polarity, substrate size, and interlayer Brønsted acidity on the specificity of the intracrystalline catalytic reaction can be controlled in part by a judicious choice of the swelling solvent.[15-17]

Among the various metal complexes that have been intercalated in clays, all are mononuclear species with the exception of group 5[34] metal clusters of the type $M_6Cl_{12}^{n+}$ with M = Nb, Ta and n = 2,3.[18] However, the intercalation of a catalytically active metal cluster species has not yet been achieved. Our recent efforts to intercalate a protonated carbonyl cluster such as $HOs_3(CO)_{12}^+$ resulted, instead, in the surface deprotonation of the cation and the selective immobilization of the neutral $Os_3(CO)_{12}$ cluster at the external hydroxylated edge sites of the silicate layers.[19] Earlier studies in our laboratory[16,20] demonstrated that neutral metal phosphine catalysts can be converted to cationic analogues by replacing the phosphine ligands with a positively charged ligand such as the phosphonium–phosphine $Ph_2P(CH_2)_2P^+Ph_2(CH_2PPh)$,[21] henceforth abbreviated $P\text{–}P^+$. In the present work, we make use of $P\text{–}P^+$ to replace a discrete number of carbonyl ligands in several metal cluster complexes to form cationic mixed-carbonyl–phosphine derivatives suitable for intercalation in hectorite, a typical smectite clay. In addition, one of the intercalated metal clusters, namely $H_2Os_3(CO)_9(P\text{–}P^+)$, has been examined as an olefin isomerization catalyst.

Experimental Section

Materials. Natural sodium hectorite (San Bernardine County, CA) having an idealized anhydrous unit cell formula of $Na_{0.67}[Mg_{5.33}Li_{0.67}](Si_{8.00})O_{20}(OH,F)_4$ was obtained in spray-dried form from the Source Clay Mineral Repository, University of Missouri. The mineral was suspended in water (1 wt %) and allowed to sediment to remove carbonate impurities. The clay fraction containing particles less than 2 μm was collected, saturated with Na^+ ions by the addition of sodium chloride, dialyzed, and freeze-dried. The cation-exchange capacity of the hydrated mineral was 70 ± 3 mequiv/100 g, as determined from Cu^{2+} binding studies.[17] $Os_3(CO)_{12}$, $Ru_3(CO)_{12}$, $H_4Ru_4(CO)_{12}$, and $Ir_4(CO)_{12}$ were used as received from Strem Chemicals Inc. $H_2Os_3(CO)_{10}$ was prepared according to a method described by Kaesz and co-workers.[22] $Me_3NO{\cdot}2H_2O$ was purchased from Aldrich Chemical Co. and was used without further purification. All solvents were reagent grade and were deoxygenated by standard freeze–vacuum–thaw cycles. 1-Hexene was obtained from Aldrich Chemical Co. and was freshly distilled over activated Al_2O_3 under an argon atmosphere prior to use as a substrate.

$(Ph_2PCH_2{}^1CH_2{}^2PPh_2CH_2{}^3Ph)(BF_4)$. The tetrafluoroborate salt of the ligand was prepared by alkylation of $Ph_2P(CH_2)_2PPh_2$ according to previously reported procedures.[20] ^1H NMR ($CDCl_3$): $\delta(H^1)$ 2.55 m, $\delta(H^2)$ 1.97 m, $\delta(H^3)$ 4.26 d ($J_{H^3P^+}$ = 14.6 Hz).

$[Ru_3(CO)_9(P\text{–}P^+)_3][BF_4]_3$. $Ru_3(CO)_{12}$ (200 mg, 0.313 mmol) and $(P\text{–}P^+)BF_4$ (542 mg, 0.939 mmol) were refluxed in 100 mL of methanol for 6 h, in a manner analogous to that described by Piacenti et al.[23] for the preparation of $Ru_3(CO)_9(PPh_3)_3$. The solvent was evaporated under vacuum, and the residue was washed with hexane to remove unreacted $Ru_3(CO)_{12}$. The residue was then treated with a minimum amount of acetone to dissolve the $[Ru_3(CO)_9(P\text{–}P^+)_3][BF_4]_3$ reaction product, and the unreacted $P\text{–}P^+$ ligand was removed by filtration. Evaporation of the acetone solution afforded the pure compound. λ_{max} (CH_2Cl_2): 489, 362 (sh) nm.

$[Os_3(CO)_{11}(P\text{–}P^+)][BF_4]$. This compound was prepared by reaction of stoichiometric amounts of $Os_3(CO)_{11}(CH_3CN)$[24] (200 mg, 0.217

---

(1) Ugo, R. *Catal. Rev.* **1975**, *11*, 225.

(2) Muetterties, E. L.; Rhodin, T. N.; Band, E.; Brucker, C. F.; Pretzer, W. R. *Chem. Rev.* **1979**, *79*, 91.

(3) (a) Gates, B. C.; Lieto, J. *CHEMTECH* **1980**, 195. (b) Gates, B. C.; Lieto, J. *CHEMTECH* **1980**, 248.

(4) Brown, S. C.; Evans, J. *J. Mol. Catal.* **1981**, *11*, 143.

(5) Castrillo, T.; Knozinger, H.; Wolf, M. *J. Mol. Catal.* **1981**, *11*, 151.

(6) Doi, Y.; Soga, K.; Yano, K.; Ono, Y. *J. Mol. Catal.* **1983**, *19*, 359.

(7) Gracey, B. P.; Evans, J. *J. Chem. Soc., Dalton Trans.* **1982**, 1123.

(8) Liu, D. K.; Wrighton, M. S. *J. Am. Chem. Soc.* **1982**, *104*, 898.

(9) Bentsen, J. G.; Wrighton, M. S. *Inorg. Chem.* **1984**, *23*, 512.

(10) Iwatate, K.; Dasqupta, S. R.; Schneider, R. L.; Smith, G. C.; Watters, K. L. *Inorg. Chim. Acta* **1975**, *15*, 191.

(11) Anderson, J. R.; Mainwaring, D. I. *J. Catal.* **1974**, *35*, 162.

(12) Brenner, A.; Burwell, R. L., Jr. *J. Catal.* **1978**, *52*, 353.

(13) Johnson, B. F. G.; Lewis, J. *Adv. Inorg. Chem. Radiochem.* **1981**, *24*, 225.

(14) Pinnavaia, T. J. *Science (Washington, D.C.)* **1983**, *220*, 365.

(15) Pinnavaia, T. J.; Raythatha, R.; Lee, J. G.-S.; Halloran, L. J.; Hoffman, J. F. *J. Am. Chem. Soc.* **1979**, *101*, 6891.

(16) Farzaneh, F.; Pinnavaia, T. J. *Inorg. Chem.* **1983**, *22*, 2216.

(17) Raythatha, R.; Pinnavaia, T. J. *J. Catal.* **1983**, *80*, 47.

(18) Christiano, S. P.; Wang, J.; Pinnavaia, T. J. *Inorg. Chem.* **1985**, *24*, 1222.

(19) Giannelis, E. P.; Pinnavaia, T. J. *Inorg. Chem.* **1985**, *24*, 2115.

(20) Quayle, W. H.; Pinnavaia, T. J. *Inorg. Chem.* **1979**, *18*, 2840.

(21) Ercolani, C.; Quagliano, J. V.; Vallarino, L. M. *Inorg. Chim. Acta* **1969**, *3*, 421.

(22) Knox, S. A. R.; Koepke, J. W.; Andrews, M. A.; Kaesz, H. D. *J. Am. Chem. Soc.* **1975**, *97*, 3942.

(23) Piacenti, F.; Bianchi, M.; Benedetti, E.; Braca, G. *Inorg. Chem.* **1968**, *7*, 1815.

0020-1669/85/1324-3602$01.50/0

mmol) and $(P\text{–}P^+)BF_4$ (125 mg, 0.217 mmol) in 30 mL of $CHCl_3$. The resulting precipitate was collected, washed with a minimum amount of chloroform, and vacuum-dried. λ_{max} (CH_2Cl_2): 407, 323 nm.

$[Ir_4(CO)_9(P\text{–}P^+)_3][BF_4]_3$. In a method analogous to that described by Stuntz[25] for the preparation of $Ir_4(CO)_{12-x}L_x$ type complexes, solid $Ir_4(CO)_{12}$ (300 mg, 0.272 mmol) was added to 500 mL of refluxing THF. To this solution were added $(P\text{–}P^+)BF_4$ (471 mg, 0.816 mmol) and solid $Me_3NO\cdot 2H_2O$ (91 mg, 0.816 mmol), and the mixture was heated at reflux for 10 min. The solvent was removed under vacuum, and the product was taken up in a minimum amount of acetone. The unreacted $Ir_4(CO)_{12}$ and excess ligand was removed by filtration. λ_{max} (CH_2Cl_2): 383 (sh), 301 nm.

$[H_4Ru_4(CO)_8(P\text{–}P^+)_4][BF_4]$. To a solution of $H_4Ru_4(CO)_{12}$ (200 mg, 0.269 mmol) in 100 mL of $CHCl_3$ were added $Me_3NO\cdot 2H_2O$ (119 mg, 0.108 mmol) and $(P\text{–}P^+)BF_4$ (620 mg, 0.108 mol). The solution after stirring overnight became cloudy. Reducing the volume by half under vacuum and cooling gave $[H_4Ru_4(CO)_8(P\text{–}P^+)_4][BF_4]$ as a precipitate. Filtering and washing the precipitate with $CHCl_3$ afforded the pure compound. λ_{max} (CH_2Cl_2): 404, 309 (sh) nm. ^1H NMR ($Me_2SO\text{-}d_6$): $\delta(\mu\text{-H})$ −16.50 (quintet) ($J_{P\text{-}H} = 7.0$ Hz).

$H_2Os_3(CO)_{10}(Ph_2PCH_2{}^1CH_2{}^2PPh_2CH_2{}^3Ph)[BF_4]$. To a solution of $H_2Os_3(CO)_{10}$ in $CHCl_3$ was added a stoichiometric amount of $(P\text{–}P^+)BF_4$, according to a method analogous to that reported for the preparation of $H_2Os_3(CO)_{10}(PPh_3)$.[26] The precipitate formed after stirring for 0.5 h was collected on a frit, washed with $CHCl_3$, and vacuum-dried. λ_{max} (CH_2Cl_2): 385, 331 nm. ^1H NMR (room temperature, $CDCl_3$): $\delta(H^1)$ 2.94 m, $\delta(H^2)$ 2.41 m, $\delta(H^3)$ 4.42 d ($J_{H^3P^+} = 13.59$ Hz) ^1H NMR (−61 °C, $CDCl_3$): $\delta(H\text{–}Os)$ −10.36 s, $\delta(\mu\text{-H})$ −20.48 m. Anal. Calcd for $C_{43}H_{33}BF_4P_2Os_3$: C, 36.06; H, 2.31; P, 4.32. Found: C, 35.69; H, 2.36; P, 3.29.

$[H_2Os_3(CO)_9(Ph_2PCH_2{}^1CH_2{}^2PPh_2CH_2{}^3Ph)][BF_4]$. A solution of $[H_2Os_3(CO)_{10}(P\text{–}P^+)]$ was refluxed in methanol under argon for 2 h, during which time the color changed from yellow to deep green. Removal of the solvent under vacuum and recrystallization from CH_2Cl_2–hexane afforded $[H_2Os_3(CO)_9(P\text{–}P^+)][BF_4]$ in the form of shiny flakes. λ_{max} (CH_2Cl_2): 359, 304 nm. ^1H NMR ($CDCl_3$): $\delta(H^1)$ 2.96 m, $\delta(H^2)$ 2.43, $\delta(H^3)$ 4.48 d ($J_{H^3P^+} = 14.26$ Hz), $\delta(\mu\text{-H})$ −11.06 d ($J_{H\text{-}P} = 7.25$ Hz).

Hectorite–Metal Cluster Complexes. In a typical experiment Na^+–hectorite (0.1 g, 0.070 mequiv) in 10 mL of water was added with stirring to a solution of the appropriate carbonyl complex (0.070 mequiv) dissolved in the minimum amount of acetone. Upon contacting the metal cluster solution, the clay immediately flocculated and took on the color of the cluster complex. After a reaction time of 10 min, the product was collected by centrifugation, washed several times with acetone to remove physically adsorbed cluster, and air-dried.

$H_2Os_3(CO)_9(P\text{–}P^+)$-Hectorite. Decarbonylation of $H_2Os_3(CO)_{10}(P\text{–}P^+)$-hectorite was achieved by heating the mineral at 80 °C under vacuum for 2 h. λ_{max} (mull): 362, 315 nm.

$HOs_3(CO)_9(CH{=}CH_2)(P\text{–}P^+)$-Hectorite. $H_2Os_3(CO)_9(P\text{–}P^+)$-hectorite (50 mg) was suspended in 50 mL of acetone, and acetylene gas, which had been passed through a trap at −78 °C, was bubbled gently at ambient temperature and pressure for 2 h. The mineral changed in color from green to bright yellow. The solvent was drawn off, and the clay was washed with acetone and dried in air.

Catalytic Reactions. $H_2Os_3(CO)_9(P\text{–}P^+)$-hectorite (30 mg, 0.010 mmol), or an equivalent amount of $H_2Os_3(CO)_9(P\text{–}P^+)[BF_4]$, was added to 5 mL of the appropriate solvent in a 15 × 150 mm Pyrex culture tube fitted with a Teflon-lined screw cap and magnetic stir bar. To the suspension was added freshly distilled 1-hexene (1.0–3.5 mL, 8.0–28 mmol). The reaction mixture was stirred at ambient temperature and pressure or the tubes were emersed in an oil bath maintained at 75 ± 0.5 °C. The temperature of the oil bath was controlled with the aid of a temperature controller (Parr Instrument Co., Model 4831) attached to an iron–constantan thermocouple. Catalytic activity was determined by withdrawing periodically a fraction of reaction solution and analyzing the products by GLC.

Physical Methods. Infrared spectra were recorded on a Perkin-Elmer Model 283B or 475 grating spectrophotometer. Solution spectra were obtained with use of 0.1-mm NaCl cells. Solutions of the cluster complexes could be prepared in the open atmosphere without noticeable spectroscopic changes over brief periods of aging (24 h). Spectra of various clay intercalates were recorded by either mixing the samples with KBr and pressing into a disk or using self-supported films. The aforementioned films were prepared by allowing an aqueous suspension of the mineral to evaporate on a polyethylene surface and then peeling away the clay. X-ray 001 basal spacings were determined on a Siemens X-ray diffractometer utilizing Ni-filtered Cu Kα radiation. Oriented film samples were prepared by evaporating aqueous suspensions of intercalated clays on microscopy slides. UV–visible spectra were recorded on a Varian Associates Cary 17 spectrophotometer. Spectra of mineral samples were prepared by mulling in mineral oil and placing the mull between silica disks. A mull sample of native hectorite was placed in the reference beam to compensate for scattering. Proton NMR spectra of carbonyl complexes were obtained with a Bruker WM-250 spectrometer with shifts reported relative to an internal reference of Me_4Si. Gas chromatography of catalytic reaction products was performed with a Varian Associates Model 920 chromatograph equipped with a thermal conductivity detector or a Hewlett-Packard Model 5880 A chromatograph equipped with a flame ionization detector. The columns were a 10 ft × $^1/_8$ in. 10% UCW on 80–100 mesh Chromosorb W and a capillary column 12.5 m × 0.2 mm containing cross-linked dimethylsilicone. Elemental analyses of the clay-intercalated complexes were performed by Schwarzkopf Microanalytical Laboratories, Woodside, NY.

Results and Discussion

Synthesis of Metal Cluster Cations. The metal cluster cations $Ru_3(CO)_9(P\text{–}P^+)_3$ and $H_2Os_3(CO)_{10}(P\text{–}P^+)$ were prepared as BF_4^- salts by the reaction of the parent carbonyl with a stoichiometric amount of $P\text{–}P^+$ according to eq 1 and 2. Coordinatively unsaturated $H_2Os_3(CO)_9(P\text{–}P^+)$ was obtained from $H_2Os_3(CO)_{10}(P\text{–}P^+)$ by decarbonylation in methanol at elevated temperatures as shown in eq 3. These reactions are analogous to those used previously[23,26,27] to prepare corresponding complexes with neutral phosphine ligands.

$$Ru_3(CO)_{12} + 3P\text{–}P^+ \xrightarrow[MeOH]{\Delta} Ru_3(CO)_9(P\text{–}P^+)_3 + 3CO \qquad (1)$$

$$H_2Os_3(CO)_{10} + P\text{–}P^+ \xrightarrow{CHCl_3} H_2Os_3(CO)_{10}(P\text{–}P^+) \qquad (2)$$

$$H_2Os_3(CO)_{10}(P\text{–}P^+) \xrightarrow[MeOH]{\Delta} H_2Os_3(CO)_9(P\text{–}P^+) + CO \qquad (3)$$

As shown by eq 4, $Ir_4(CO)_9(P\text{–}P^+)_3$ was obtained as the BF_4^- salt from $Ir_4(CO)_{12}$ and $P\text{–}P^+$ in the presence of Me_3NO as a decarbonylation reagent. A related pathway, illustrated by eq 5 and 6, was used to prepare $Os_3(CO)_{11}(P\text{–}P^+)$.

$$Ir_4(CO)_{12} + 3P\text{–}P^+ + 3Me_3NO \xrightarrow{THF} Ir_4(CO)_9(P\text{–}P^+)_3 + 3CO_2 + 3Me_3N \qquad (4)$$

$$Os_3(CO)_{12} + Me_3NO \xrightarrow[CH_2Cl_2]{CH_3CN} Os_3(CO)_{11}(CH_3CN) + CO_2 + Me_3N \qquad (5)$$

$$Os_3(CO)_{11}(CH_3CN) + P\text{–}P^+ \xrightarrow{CHCl_3} Os_3(CO)_{11}(P\text{–}P^+) + CH_3CN \qquad (6)$$

These synthetic pathways parallel those developed previously[24,25] for the synthesis of mixed metal cluster carbonyls containing triphenylphosphine and related neutral phosphine ligands. Thus the reactivity of $P\text{–}P^+$ toward metal cluster centers is very similar to the reactivity of arylphosphine ligands.

Although $H_4Ru_4(CO)_8L_4$ type species have been obtained from $H_4Ru_4(CO)_{12}$ by ligand exchange with the appropriate phosphine ligand[28] the reaction is usually accompanied by the formation of other mixed-ligand complexes. Thus, in the present work Me_3NO was used to achieve the quantitative displacement of four carbonyl ligands from $H_4Ru_4(CO)_{12}$ according to eq 7.

$$H_4Ru_4(CO)_{12} + 4P\text{–}P^+ + 4Me_3NO \xrightarrow{CHCl_3} H_4Ru_4(CO)_8(P\text{–}P^+)_4 \qquad (7)$$

The CO stretching frequencies in the infrared spectra of mixed-ligand metal cluster carbonyls are diagnostic of the constitution of the complex. Table I compares the CO frequencies of the above metal cluster cations with those for analogous com-

---

(24) Johnson, B. F. G.; Lewis, J.; Pippard, D. A. *J. Chem. Soc., Dalton Trans.* **1981**, 407.

(25) Stuntz, G. F. Ph.D. Thesis, University of Illinois, 1978.

(26) Deeming, A. J.; Hasso, S. *J. Organomet. Chem.* **1976**, *114*, 313.

(27) Bruce, M. I.; Shaw, G.; Stone, F. G. A. *J. Chem. Soc., Dalton Trans.* **1972**, 2094.

(28) Piacenti, F.; Bianchi, M.; Frediani, P.; Benedetti, E. *Inorg. Chem.* **1971**, *10*, 2759.

Table I. Infrared CO Stretching Frequencies (cm^{-1}) for Metal Cluster Carbonyls Containing Positively Charged and Neutral Phosphine Ligands

complex	L = P–P^{+a}	L = PPh$_3$^{b}	L = Ph$_2$C$_2$H$_4$Si(OEt)$_3$^{b}	ref
$Ru_3(CO)_9L_3$	2048 m, 1980 s, 1962 s	2044 vw, 1978 sh, 1967 s	2044 m, 1970 s, 1940 s	8, 27
$H_4Ru_4(CO)_8L_4$	2005 s, 1971 m, 1948 s	2015 s, 1984 m, 1952 m, 1930 w	2008 s, 1981 m, 1948 s, 1920 w	6, 28
$Ir_4(CO)_9L_3$	2039 m, 1995 sh, 1984 s, 1965 sh, 1832 vw, 1779 s	2047 m, 2038 sh, 1992 s, 1973 sh, 1799 s, 1787 sh		25
$Os_3(CO)_{11}L$	2100 m, 2048 s, 2028 s, 2010 vs, 1998 sh, 1983 m, 1976 m	2108 m, 2055 s, 2035 s, 2019 s, 2000 m, 1989 m, 1978 m		24
$H_2Os_3(CO)_{10}L$	2100 m, 2060 s, 2042 s, 2018 vs, 1990 sh, 1976 m, 1960 m	2105 m, 2066 s, 2051 s, 2025 vs, 2017 vs, 2004 m, 1983 m, 1971 m	2106 m, 2066 s, 2051 s, 2025 vs, 2007 sh, 1983 m, 1972 m	9, 26
$H_2Os_3(CO)_9L$	2090 m, 2050 s, 2001 vs, 1989 s, 1948 m	2093 m, 2053 s, 2015 sh, 2012 vs, 2004 m, 1991 m, 1976 m, 1962 w	2091 m, 2052 s, 2012 vs, 1988 s, 1974 m, 1954 w	9, 26

[a] Complexes containing P–P$^+$ are BF$_4^-$ salts in CH$_2$Cl$_2$ solution. [b] Frequencies for complexes containing neutral phosphine ligands were obtained from the references provided.

plexes containing neutral phosphine ligands. In each case, good agreement is found between the cationic and neutral species.

Ion-Exchange Reactions. Initial attempts to exchange the interlayer Na$^+$ ions in hectorite with P–P$^+$ metal cluster complexes in various organic solvents were unsuccessful. The resulting products after being dried in air exhibited 001 X-ray spacings of about 12.6 Å, indicative of Na$^+$–hectorite containing a monolayer of interlayer water. Interestingly, the products were colored and exhibited weak terminal CO stretching frequencies characteristic of the starting metal cluster complex. This suggests that some cluster cations were immobilized by ion exchange on the *external* surfaces of the clay particles.

The little or no exchange between interlayer Na$^+$ ions and cluster cations in organic solvents can be explained in terms of the swelling properties of the initial clay.[29] Although organic solvents such as CH$_2$Cl$_2$, acetone, and others swell Na$^+$–hectorite, the expansion of the interlayer space is generally limited to ≤ 10 Å. This limited swelling makes it difficult for the bulky metal cluster complex to penetrate the interlayer and displace Na$^+$. In other words, the process expressed in eq 8, wherein the heavy lines

$$\overline{\underline{n\mathrm{Na}^+}} + \mathrm{M}_m{}^{n+} \xrightarrow[\text{solvent}]{\text{organic}} \overline{\underline{\mathrm{M}_m{}^{n+}}} + n\mathrm{Na}^+ \qquad (8)$$

represent the silicate layers and M$_m{}^{n+}$ the cluster cations, is exceedingly slow. However, the Na$^+$ ions at external basal planes or at edges containing broken bonds[30] are readily replaced, accounting for the color changes and the appearance of weak CO stretching frequencies.

Despite the above limitations encountered in organic solvents, exchange of interlayer Na$^+$ by metal cluster complexes could be achieved by first suspending the clay in water and then adding this suspension to an acetone solution of metal cluster cation. Earlier studies of the colloidal and rheological properties of aqueous Na$^+$–smectite suspensions[29] indicate that the clay layers are highly swollen and largely delaminated in aqueous suspension. Under these conditions the Na$^+$ ions on the basal surfaces are readily available for ion exchange. This is in contrast to the situation expressed in eq 8, where the clay layers are initially oriented face to face. Upon the addition of the clay suspension to the cluster cation solution, the Na$^+$ ions are replaced and the silicate layers reorient themselves in a face to face fashion. The overall process can be represented schematically as shown in eq 9.

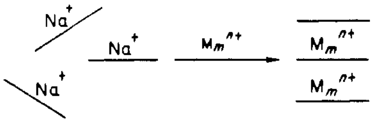

(9)

Except for H$_2$Os$_3$(CO)$_9$(P–P$^+$) and HOs$_3$(CO)$_9$(CH=CH$_2$)(P–P$^+$), all metal cluster complexes containing P–P$^+$ were intercalated in hectorite by ion exchange according to eq 9.

Table II. Analytical Data for Hectorite-Intercalated Metal Cluster Complexes

intercalated cation	wt % M	wt % P	mequiv of complex/100 g of clay	M/P mole ratio found	M/P mole ratio calcd
$H_4Ru_4(CO)_8(P\text{–}P^+)_4$	4.32	2.41	60	0.53	0.50
$Ru_3(CO)_9(P\text{–}P^+)_3$	5.47	2.89	83	0.57	0.50
$Ir_4(CO)_9(P\text{–}P^+)_3$	9.72	2.39	49	0.66	0.67
$H_2Os_3(CO)_9(P\text{–}P^+)^a$	19.27	2.17	62	1.45	1.50
$Os_3(CO)_{11}(P\text{–}P^+)$	10.92	1.31	26	1.37	1.50

[a] This intercalated cluster was formed by decarbonylation of H$_2$Os$_3$(CO)$_{10}$(P–P$^+$)–hectorite containing a comparable metal loading.

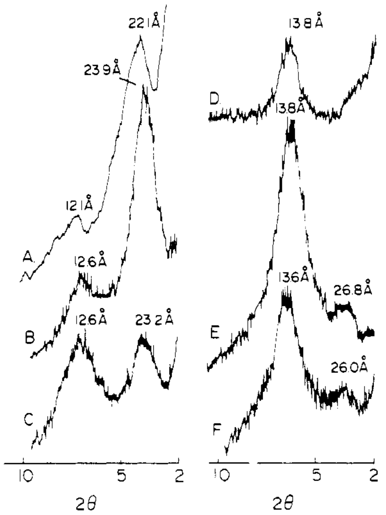

Figure 1. X-ray diffraction patterns (Cu Kα) of hectorite intercalated with metal cluster cations: (A) Ru$_3$(CO)$_9$(P–P$^+$)$_3$; (B) H$_4$Ru$_4$(CO)$_8$(P–P$^+$)$_4$; (C) Ir$_4$(CO)$_9$(P–P$^+$)$_3$; (D) Os$_3$(CO)$_{11}$(P–P$^+$); (E) H$_2$Os$_3$(CO)$_{10}$(P–P$^+$); (F) H$_2$Os$_3$(CO)$_9$(P–P$^+$). Samples were prepared as oriented films on glass slides to favor the 00*l* reflections.

H$_2$Os$_3$(CO)$_9$(P–P$^+$)–hectorite was obtained by decarbonylation of H$_2$Os$_3$(CO)$_{10}$(P–P$^+$)–hectorite at 80 °C in vacuo. HOs$_3$(CO)$_9$(CH=CH$_2$)(P–P$^+$)–hectorite was prepared by reaction of H$_2$Os$_3$(CO)$_9$(P–P$^+$)–hectorite with acetylene in acetone (cf. Experimental Section).

Table II summarizes the loadings obtained for each metal cluster cation. In each case the observed metal to phosphorus ratio is in acceptable agreement with the value expected from the idealized formulas. The metal loadings reported in the table correspond to 32–100% of the cation-exchange capacity of the clay.

The intercalation of metal cluster cations in hectorite results in 001 spacings in the range 22–27 Å. Since the van der Waals thickness of a layer is approximately 9.5 Å, the 001 spacings correspond to interlayer thicknesses or gallery heights of 12.5–17.5 Å. Typical diffraction patterns for oriented film samples are shown in Figure 1. In general, the line profiles are similar to those of the native clay and only two orders of 001 refections are observed.

---

(29) Van Olphen, H. "An Introduction to Clay Colloid Chemistry", 2nd ed.; Wiley: New York, **1977**; Chapter 7.

(30) Borchard, G. A. In "Minerals in Soil Environments"; Dixon, J. B., Weed, S. B., Eds.; Soil Science of America: Madison, WI, **1977**; Chapter 9.

Table III. Spectral Data for Metal Cluster Complexes Intercalated in Hectorite

intercalated complex	λ(max), nm[a]	ν(CO), cm^{-1} [b]
$Ru_3(CO)_9(P\text{–}P^+)_3$	497, 360 sh	2042 m, 1970 s, 1960 sh
$H_4Ru_4(CO)_8(P\text{–}P^+)_4$	417, 310 sh	2002 s, 1965 sh, 1946 s
$Ir_4(CO)_9(P\text{–}P^+)_3$	380 sh, 290	2038 m, 1995 sh, 1980 vs, 1965 sh, 1835 vw, 1877 s
$Os_3(CO)_{11}(P\text{–}P^+)$	415, 300	2102 m, 2050 s, 2025 sh, 2001 vs, 1995 sh, 1975 s
$H_2Os_3(CO)_{10}(P\text{–}P^+)$	380	2100 m, 2062 s, 2042 s, 2010 vs, 1998 sh, 1980 m, 1970 m
$H_2O_3(CO)_9(P\text{–}P^+)$[c]	362, 315	2092 m, 2052 s, 2000 vs, 1978 s, 1950 sh
$HOs_3(CO)_9(CH{=}CH_2)(P\text{–}P^+)$[d]		2090 m, 2042 s, 1999 vs, 1962 sh

[a] UV–vis spectra were obtained on mineral oil mulls. [b] Samples used for IR spectra were KBr pellets. [c] This intercalated species was formed in situ from $H_2Os_3(CO)_{10}(P\text{–}P^+)$–hectorite by heating in vacuo at 80 °C. [d] This complex was prepared in situ by reaction of $H_2Os_3(CO)_9$-$(P\text{–}P^+)$-hectorite with acetylene.

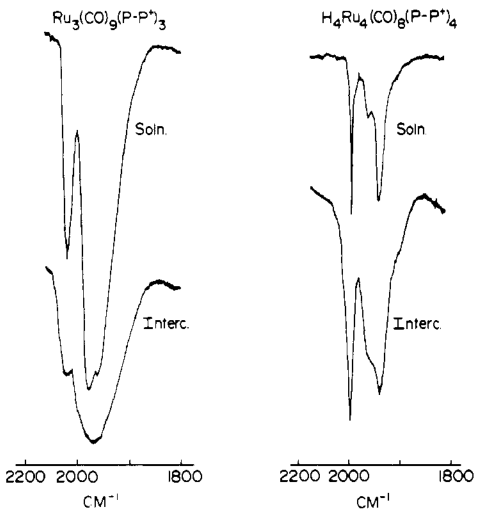

Figure 2. Infrared spectra in the CO stretching region for $Ru_3(CO)_9$-$(P\text{–}P^+)_3$ and $H_4Ru_4(CO)_8(P\text{–}P^+)_4$ dissolved in CH_2Cl_2 (BF_4^- salts) and intercalated in hectorite (KBr pellet).

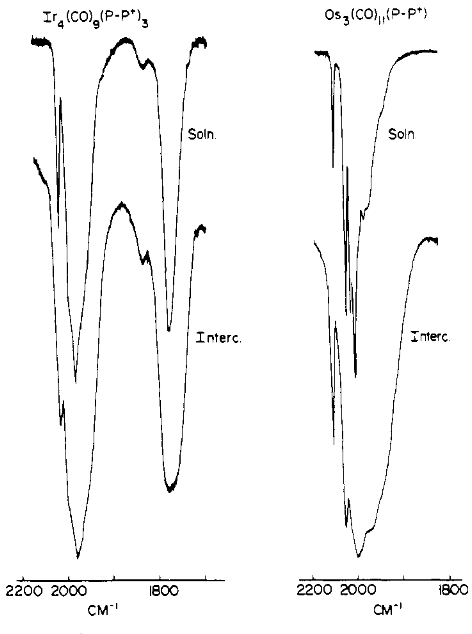

Figure 3. The CO stretching regions in the IR spectra of $Ir_4(CO)_9(P\text{–}P^+)_3$ and $Os_3(CO)_{11}(P\text{–}P^+)$ dissolved in CH_2Cl_2 (BF_4^- salts) and intercalated in hectorite (KBr pellet).

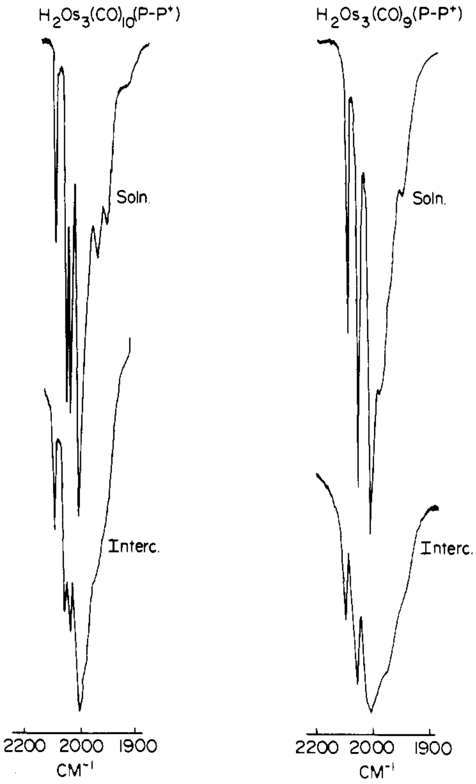

Figure 4. The CO stretching regions for $H_2Os_3(CO)_{10}(P\text{–}P^+)$ and $H_2Os_3(CO)_9(P\text{–}P^+)$ dissolved in CH_2Cl_2 (BF_4^- salts) and intercalated in hectorite (KBr pellet).

This latter result indicates that the gallery heights are not rigorously regular or, equivalently, that these intercalation compounds are interstratified. The presence of $P\text{–}P^+$ alone in the interlayers results in a 001 spacing of 18.8 Å. Thus the lattice expansions caused by intercalation of the cluster cations are due in large part to the $P\text{–}P^+$ ligands. The size and shape of the metal cluster, as well as solvation effects, also contribute to the overall lattice expansion. The relative intensities of the 001 and 002 reflections provide additional evidence for the intercalation of the cluster cations in the clay galleries. It is apparent from the patterns in Figure 1 and the data in Table II that the 001 reflection is strong for the ruthenium intercalates (samples A and B) with the lowest metal loadings and weak for the osmium intercalates (samples D–F) with the highest metal loadings. The 001 and 002 reflections are of comparable intensity for the iridium intercalate (sample C).

The carbonyl stretching frequencies for the intercalated metal cluster cations are provided in Table III, along with the positions of absorption maxima in the UV–vis spectra. Figures 2–4 provide a direct comparison of the IR spectra in the carbonyl region for the metal cluster cations in homogeneous solution and in the clay-intercalated state. Although the CO bands are broadened in the intercalated state, perhaps due to a lowering of symmetry and/or a distribution of metal cluster environments, their positions and relative intensities are very similar to those observed for the cluster cations in solution. These results indicate that the cluster cations retain their constitution in the intercalated state, as expected for a purely electrostatic guest–host interaction.

Another indication of the retention of structure for the intercalated cluster cations is provided by the electronic spectra. In general, the deviations in λ_{max} for the intercalated complex (cf. Table III) and the solution cluster (cf. Experimental Section) are small, typically less than 10 nm. These small deviations in band position could arise from differences in solvation and/or interactions of the cluster with the negatively charged silicate sheets.

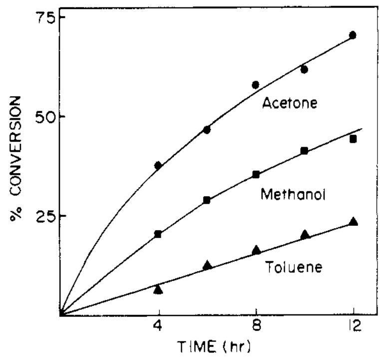

Figure 5. Conversion of 1-hexene (8.0 mmol) to *cis* and *trans*-2-hexene with hectorite-intercalated $H_2Os_3(CO)_9(P\text{–}P^+)$ (0.01 mmol) as catalyst at 25 °C. In each case the amount of solvent used was 5.0 mL.

Olefin Isomerization. Triosmium cluster complexes of the type $H_2Os_3(CO)_9L$ (L = CO, $P(aryl)_3$, $P(aryl)_2R$), whether in homogeneous solution or in the supported state, are active catalysts for the isomerization of terminal olefins.[26,31,32] These reaction systems are among the few well-characterized catalytic cycles for which the elementary steps are known to occur exclusively on the intact cluster and not on molecular fragments or metal aggregates formed from the cluster acting as a precursor. Typically, the catalytically active $H_2Os_3(CO)_9L$ species are formed from $H_2Os_3(CO)_{10}L$ by thermal decarbonylation. Since an analogous decarbonylation occurs when L = $P\text{–}P^+$, it was of interest in the present work to examine the olefin-isomerization activity of $H_2Os_3(CO)_9(P\text{–}P^+)$ in the clay-intercalated state, as well as in homogeneous solution.

Figure 5 illustrates the conversion of 1-hexene to *cis*- and *trans*-2-hexene with $H_2Os_3(CO)_9(P\text{–}P^+)$–hectorite in three different solvent systems. Under equivalent conditions in homogeneous acetone solution, the conversion after 12 h was about 95% vs. 70% for the intercalated catalyst. It is significant that the activity of the intercalated catalyst decreases with solvating medium in the order acetone > methanol > toluene. This solvent dependence parallels the swelling power of the solvents and the accessibility of the intercalated metal centers. When $P\text{–}P^+$ complexes occupy the interlayer surfaces of smectites, acetone and methanol typically expand the gallery height by approximately 6 and 3 Å, respectively.[16,20] In contrast, toluene causes little or no interlayer swelling.

The activity observed for the toluene-solvated catalyst is at least 1 order of magnitude larger than would be expected on the basis of metal cluster centers bound at external surfaces. For example, the initial 1-hexene isomerization rates for the intercalated catalyst in acetone and toluene are approximately 75 and 13 (mol/mol of cluster)/h, respectively, as estimated from the data in Figure 5. Previous studies[15] of clay-immobilized metal complex hydrogenation catalysts indicate that the ratio of reactive centers at intracrystalline gallery sites and external surface sites is at least 100:1. Presumably, the isomerization of 1-hexene in acetone by $H_2Os_3(CO)_9(P\text{–}P^+)$–hectorite occurs mainly in the solvent-swollen galleries, because the reactivities of the intercalated and homogeneous catalysts are so similar in this solvent (see above). Therefore, the reactivity of the intercalated catalyst in toluene is too high to be attributed exclusively to metal cluster sites at external surfaces. Thus, the intercalated clusters themselves act as pillars between the silicate layers, providing a gallery height of about 16 Å for diffusion of substrate to the interlayer metal cluster centers.

The intercalated catalyst could be reused for 1-hexene isomerization in acetone until the total number of catalyst turnovers approached 3300 mol of substrate/mol of cluster. At this point, catalytic activity ceases and the color of the catalyst changes from deep green to bright yellow. An analogous loss of activity and change in color occurs for the homogeneous catalyst in acetone after the same number of turnovers. The CO stretching frequencies in the IR spectra of the spent intercalated catalysts were essentially identical with those found for a saturated $HOs_3(CO)_9(\text{vinylidene})(P\text{–}P^+)$ complex formed by reaction of $H_2Os_3(CO)_9(P\text{–}P^+)$–hectorite with acetylene (cf. Table III). These observations are consistent with previously reported studies which attribute the loss of activity of $H_2Os_3(CO)_9L$ catalysts to the formation of saturated complexes containing a bridging vinylidene ligand.[31]

In a related series of experiments the isomerization of 1-hexene by $H_2Os_3(CO)_9(P\text{–}P^+)$–hectorite in toluene was observed at 75 °C. No catalyst decomposition was observed during the course of the reaction. The rate of the reaction was found to be proportional to the concentration of olefin as well as the concentration of the catalyst, in agreement with results obtained by Gates and co-workers[31] for 1-pentene isomerization in the presence of $H_2Os_3(CO)_{10}$ in toluene at 75 °C. In the same report these workers observed that the related silica-supported $H_2Os_3(CO)_9L$ catalyst was more stable than its homogeneous analogue, yielding approximately 10^3 mol of internal olefin/mol of cluster prior to catalyst cessation. In our study, both the intercalated and homogeneous $H_2Os_3(CO)_9(P\text{–}P^+)$ catalyst exhibit a turnover number of 3300 mol of 1-hexene/mol of cluster in acetone at 25 °C. This value is more than 3 times as large as the value reported for the related silica-supported triosmium cluster. The similarities between the homogeneous and intercalated metal cluster catalysts are additional evidence that molecular complexes electrostatically immobilized in solution-like solvated clay interlayers retain their catalytic properties.

Finally, we should note that, during the course of 1-hexene isomerization in methanol, a small amount of the intercalated metal complex is desorbed into solution. However, no desorption of osmium was observed when acetone or toluene was the solvating medium. Since electrical neutrality must be maintained within the clay, the desorbed complex in methanol most likely is a neutral species as depicted in eq 10. To investigate further the role of

$$\overline{\underline{H_2Os_3(CO)_9(P\text{-}P^+)}} \xrightarrow{\text{MeOH}} \overline{\underline{P\text{-}P^+}} + [\text{metal cluster carbonyl}]_{\text{soln}} \quad (10)$$

methanol, we examined the desorption of cluster from hectorite in the absence of substrate. After clay suspension was stirred overnight in methanol, the color of the mineral changed from green to yellow, and a portion of the cluster was desorbed into the solution. No isomerization to internal olefin was observed when 1-hexene was added to this slurry. Furthermore, the spectrum of the filtrate exhibited terminal CO bands at 2113 w, 2090 m, 2051 m, 2002 vs, and 1940 m cm^{-1} and no absorptions characteristic of the $P\text{–}P^+$ ligand. The complex IR pattern suggests that a metal cluster structure was retained by the desorbed complex. The coordination of methanol by tungsten subcarbonyls formed by the photochemical displacement of CO from $W(CO)_6$ has been proposed previously.[33] It may be that a similar complexation process is operating in the displacement of the $P\text{–}P^+$ ligand from the intercalated osmium cluster.

Conclusions

Our results demonstrate that the reactivity of $P\text{–}P^+$ toward osmium, ruthenium, and iridium cluster carbonyls parallels the reactivity of neutral arylphosphines. Thus $P\text{–}P^+$ is a useful reagent for preparing cationic metal cluster complexes suitable for intercalation in smectite clays. These results are compatible with our earilier findings for mononuclear $RhCl(COD)(P\text{–}P^+)$ and $RhCl(CO)(P\text{–}P^+)_2$ complexes, which can also be isolated as salts and intercalated in smectite clays as catalyst precursors for olefin

---

(31) Freeman, M. B.; Patrick, M. A.; Gates, B. C. *J. Catal.* **1982**, *73*, 82.

(32) Effa, J. B. N.; Lieto, J.; Aune, J. P. *J. Mol. Catal.* **1981**, *62*, 149.

(33) Lee, A. J.; Adamson, A. W. *J. Am. Chem. Soc.* **1982**, *104*, 3804.

(34) In this paper the periodic group notation is in accord with recent actions by IUPAC and ACS nomenclature committees. A and B notation is eliminated because of wide confusion. Groups IA and IIA become groups 1 and 2. The d-transition elements comprise groups 3 through 12, and the p-block elements comprise groups 13 through 18. (Note that the former Roman number designation is preserved in the last digit of the new numbering: e.g., III → 3 and 13.)

hydrogenation and hydroformylation.

The intercalation of metal clusters containing P–P$^+$ in hectorite is governed mainly by the accessibility of Na$^+$ exchange ions on the basal surfaces. Since the swelling of the clay by organic solvents is limited, the size of the metal cluster complex exceeds the initial gallery height of the clay and the rate of intercalation is low. However, if the clay is swollen and largely delaminated by dispersion in water, then the Na$^+$ ions on the basal surfaces are readily accessible for exchange and ordered intercalation compounds are formed upon face to face flocculation of the silicate layers in the presence of the cluster cations.

$H_2Os_3(CO)_9(P{-}P^+)$–hectorite, the first reported example of an intercalated metal cluster catalyst, is active for the isomerization of 1-hexene in solvents that swell the clay interlayers (e.g., acetone and methanol), as well as in solvents that are nonswelling (e.g., toluene). The activity in nonswelling solvents is attributed to a pillaring effect which leads to a large gallery height (~16 Å) and allows for the interlayer penetration of the substrate. The longevity of the intercalated catalyst parallels that of the homogeneous catalyst, further indicating that the metal cluster complex retains solution-like properties in the intercalated state.

Acknowledgment. The partial support of this research by the National Science Foundation through Grant CHE-8306583 is gratefully acknowledged.

Registry No. $(P{-}P^+)(BF_4)$, 71243-21-5; $[Ru_3(CO)_9(P{-}P^+)_3][BF_4]_3$, 97920-21-3; $[Os_3(CO)_{11}(P{-}P^+)][BF_4]$, 97920-23-5; $[Ir_4(CO)_9(P{-}P^+)_3][BF_4]_3$, 97950-39-5; $[H_4Ru_4(CO)_8(P{-}P^+)_4][BF_4]$, 97920-25-7; $[H_2Os_3(CO)_{10}(P{-}P^+)][BF_4]$, 97920-27-9; $[H_2Os_3(CO)_9(P{-}P^+)][BF_4]$, 97920-29-1; $Ru_3(CO)_{12}$, 15243-33-1; $Os_3(CO)_{11}(CH_3CN)$, 65702-94-5; $Ir_4(CO)_{12}$, 18827-81-1; $H_4Ru_4(CO)_{12}$, 34438-91-0; $H_2Os_3(CO)_{10}$, 41766-80-7; $[HOs_3(CO)_9(CH{=}CH_2)(P{-}P^+)]^+$, 97950-40-8; acetylene, 74-86-2; hectorite, 12173-47-6.

Contribution from the Department of Synthetic Chemistry, Faculty of Engineering,
The University of Tokyo, Hongo, Bunkyo-ku, Tokyo 113, Japan

Importance of an Axially Orientated *C*-Methyl Group in the Stereospecific Formation of the Λ-β-(Oxalato)((4*R*,6*R*)-4,6-dimethyl-3,7-diaza-1,9-nonanediamine)cobalt(III) Ion

MORIO YASHIRO, SHIGENOBU YANO,* MASANOBU AJIOKA, and SADAO YOSHIKAWA*

Received February 13, 1985

cis-[Co(ox)(5*S*-Me-2,3,2-tet)]$^+$ (5*S*-Me-2,3,2-tet = (*S*)-4-methyl-3,7-diaza-1,9-nonanediamine) has been newly synthesized. Two stereoisomers, Λ-β- and Δ-β-[Co(ox)(5*S*-Me-2,3,2-tet)]$^+$, have been obtained and characterized by elementary analyses and by ^{1}H and ^{13}C NMR, absorption, and circular dichroism spectroscopies. The distribution of these isomers at thermodynamic equilibrium has been examined in order to elucidate roles of the two *C*-methyl groups in the stereospecific formation of Λ-β-[Co(ox)(5*R*,7*R*-Me$_2$-2,3,2-tet)]$^+$ (5*R*,7*R*-Me$_2$-2,3,2-tet = (4*R*,6*R*)-4,6-dimethyl-3,7-diaza-1,9-nonanediamine). Factors of the stereospecific formation of Λ-β-[Co(ox)(5*R*,7*R*-Me$_2$-2,3,2-tet)]$^+$ are discussed in relation to the predictions of the strain energy minimization calculations. The results suggest that the existence of the equatorially orientated *C*-methyl group of the tetraamine is not the essential factor, but the axially orientated *C*-methyl group plays an important role in the occurrence of the stereospecificity.

Introduction

As a source of asymmetry in asymmetric syntheses, the utility of chiral transition-metal complexes has been of current interest. We have previously developed a cyclic system for asymmetric syntheses of α-amino acids[1] using a chiral cobalt(III) complex containing an optical active tetraamine, 1,5*R*,7*R*,11-Me$_4$-2,3,2-tet.[2] In the system, the stereospecific feature of 5*R*,7*R*-Me$_2$-2,3,2-tet[3] which binds to the cobalt(III) center only in the Λ-cis-β form[4] has been applied fundamentally in order to provide two chiral coordination sites. A close investigation of the factors related to the appearance of this remarkable stereospecificity should provide important information in designing ligands suitable for metal-assisted asymmetric syntheses. However, no study has discussed the factors of the appearance of this stereospecificity. Therefore, this work is aimed at clarifying the origin of this stereospecificity of the tetraamine.

Our other X-ray studies of the *cis* cobalt(III) complexes containing 5*R*,7*R*-Me$_2$-2,3,2-tet or 1,5*R*,7*R*,11-Me$_4$-2,3,2-tet have shown that the central six-membered chelate ring of the tetraamine ligand adopts the chair conformation with one methyl group axial and the other equatorial.[1,5,6] Formation of the two diastereoisomers, Λ-β or Δ-β, is determined by which of the two terminal five-membered chelate rings links to the apical position (Figure 1). It is a striking feature that the Λ-β isomer is stereospecifically obtained although the skeleton of the six-membered chelate ring takes the achiral chair conformation. It seems that the axially orientated *C*-methyl group on the six-membered chelate ring plays an important role in the appearance of the remarkable stereospecificity of the tetraamine. In this investigation, in order to elucidate the role of the axially orientated *C*-methyl group of the tetraamine, we have newly prepared *cis*-[Co(ox)(5*S*-Me-2,3,2-tet[7,8])]$^+$, which is expected to have the structure that may result from removing the axially orientated *C*-methyl group from *cis*-[Co(ox)(5*R*,7*R*-Me$_2$-2,3,2-tet)]$^+$, and have examined its stereochemistry.

In addition, in order to evaluate factors of the appearance of the remarkable stereospecificity in more detail, we have performed strain energy minimization calculations for four related complex ions: Λ-β-[Co(ox)(5*R*-Me-2,3,2-tet)]$^+$, Δ-β-[Co(ox)(5*R*-Me-2,3,2-tet)]$^+$, Λ-β-[Co(ox)(5*R*,7*R*-Me$_2$-2,3,2-tet)]$^+$, and Δ-β-[Co(ox)(5*R*,7*R*-Me$_2$-2,3,2-tet)]$^+$.

Experimental Section

Measurements. Absorption spectra were obtained on a Shimadzu UV-210 double-beam spectrophotometer. Circular dichroism spectra were obtained on a JASCO J-500A spectropolarimeter. These measurements were made on aqueous solutions at concentrations near 2×10^{-3} M.

^{1}H NMR spectra were obtained on a JEOL GX-400 instrument (400 MHz) with sodium 3-(trimethylsilyl)propanesulfonate as an internal reference in D$_2$O.

---

(1) Ajioka, M.; Yano, S.; Matsuda, K.; Yoshikawa, S. *J. Am. Chem. Soc.* **1981**, *103*, 2459.

(2) The fully systematic name is (6*R*,8*R*)-6,8-dimethyl-2,5,9,12-tetraazatridecane.

(3) The fully systematic name is (4*R*,6*R*)-4,6-dimethyl-3,7-diaza-1,9-nonanediamine.

(4) Mizukami, F. *Bull. Chem. Soc. Jpn.* **1975**, *48*, 472.

(5) Yano, S.; Fujioka, A.; Yamaguchi, M.; Yoshikawa, S. *Inorg. Chem.* **1978**, *17*, 14.

(6) Yashiro, M.; Ajioka, M.; Yano, S.; Toriumi, K.; Ito, T.; Yoshikawa, S., submitted for publication.

(7) The fully systematic name is (*S*)-4-methyl-3,7-diaza-1,9-nonanediamine.

(8) In order to compare with the 5*R*,7*R*-Me$_2$-2,3,2-tet system clearly, in place of the *S* form, upon which we actually experimented, its enantiomer (*R* form) was employed to discuss.

0020-1669/85/1324-3607$01.50/0